Received: 7 October 2022 | Accepted: 21 December 2022

DOI: 10.1002/pamm.202200162

Semi-crystalline polymers at finite strains: A thermo-coupled constitutive model for varying degrees of crystallinity and temperatures

Marie-Christine Reuvers[1,*], **Birte Boes**[1], **Sebastian Felder**[1], **Tim Brepols**[1], **Sameer Kulkarni**[2], **Klara Loos**[2], **Michael Johlitz**[2], **Alexander Lion**[2], and **Stefanie Reese**[1]

[1] Institute of Applied Mechanics, RWTH Aachen University, Mies-van-der-Rohe-Str.1, 52074 Aachen
[2] Institut für Mechanik, Universität der Bundeswehr München, Werner-Heisenberg-Weg 39, 85577 Neubiberg

Thermoplastics are gaining interest for various industrial applications, since they can be widely used for thermoforming and injection moulding processes due to their thermostable material behavior. In combination with the material's low density and high strength to mass ratio, they are especially of interest in times where an improved environmental balance is more and more important. Hence, why they are for example frequently used in the automotive industry to reduce the weight of automotive components.

Semi-crystalline polymers as a subcategory of thermoplastics, partly crystallize after cool-down from the molten state. During the thermoforming process, they are subjected to large deformations as well as thermal loads and show strong thermo-mechanical coupling effects in addition to the influence of the evolution of the crystalline phase on the macroscopic material behavior. Therefore, computational models are needed to predict the complex material response reliably and minimize production errors.

This work presents a thermomechanically consistent material formulation at finite strains. In order to account for the highly nonlinear material behavior, elasto-plastic and visco-elastic contributions are combined in the Helmholtz free energy and a dependency on temperature as well as the degree of cristallinity (DOC) is incorporated. Special attention is devoted to the choice of yield function and hardening behavior.

A comparison of the simulation results to experiments at varying degrees of crystallinity and temperatures is presented to review the changes in the formulation. Therefore a special blending technique is used to ensure stable crystallinity conditions in the test samples.

1 Introduction

Thermoplastics are used in a variety of industry applications due to their temperature stability and their potential for cost-effective mass production. They can be subdivided into purely amorphous and semi-crystalline materials, depending on their microstructure. Polyamide 6 (PA 6) belongs to the category of semi-crystalline polymers due to its biphasic microstructure, that results in a complex elasto-plastic, visco-elastic material behavior on the macro level. Hereby, for example the manufacturing process, thermal treatment, applied stresses and moisture act as influencing factors, which can change the material behavior significantly [4]. Consequently, a wide range of constitutive models concerning this behavior have been established during the last decade. In the field of semi-crystalline polymers earlier works bof Haward et al. [5] and Boyce et al. [6] using a phenomenological approach laid the foundation for extended work in e.g. [7]. Anand et al. [2], Srivastava et al. [8] and Wang et al. [9] have accounted for the thermal influence on PA 6, whereas the influence of strain rate has been investigated in [10]. Finally, the influence of the degree of crystallinity has been studied in e.g. [11] and moisture was accounted for in [12], to name a few. In some works multiple influencing factors are included, as for example temperature and strain rate in [13] or thermal and moisture effects in [14], whereas Felder et al. [1, 15] modeled the influence of temperature, strain rate and crystallinity. In this work, similar to [1] a phenomenological modeling approach is chosen (see Section 2), combining an elasto-plastic and a visco-elastic contribution in parallel. The DOC in this framework serves as a constant input parameter for the fully thermocoupled model. A tension-compression asymmetric yield surface is chosen [18] to model the material's yielding behavior. Finally, the constitutive equations are derived in a thermomechanical consistent manner. After the implementation as a user subroutine UMAT into the commercial ABAQUS framework, the model is characterized in Section 3 using experimental results. Therefore, a staggered identification scheme is exploited using least-square optimization. Finally, in Section 4 the results of the identification procedure are discussed and an outlook regarding further research is given.

2 Material model

2.1 Kinematics

To describe the visco-elastic elasto-plastic material behavior of PA 6 for finite strains, the deformation gradient $\boldsymbol{F}$ is introduced alongside the right Cauchy-Green tensor $\boldsymbol{C} = \boldsymbol{F}^T\boldsymbol{F}$ as deformation measure. In line with the works of e.g. [1, 2] two decoupled processes are assumed (cf. Figure 1 a)), which motivate the split of the model into an elasto-plastic (index 1)

* Corresponding author: e-mail marie.reuvers@ifam.rwth-aachen.de, phone +00 241 80 25003, fax +00 241 80 22001

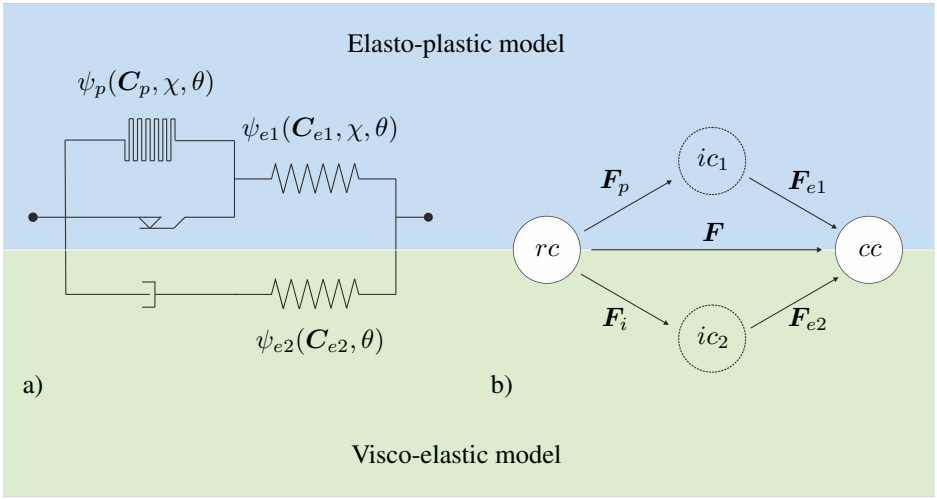

Fig. 1: a) Schematic illustration of the constitutive model b) Multiplicative splits of the deformation gradient

and a visco-elastic (index 2) contribution. Following this assumption, the deformation gradient is decomposed into an elastic and a plastic $\boldsymbol{F} = \boldsymbol{F}_{e1}\,\boldsymbol{F}_p$ part for the elasto-plastic branch. For the viscous part, this yields a split into elastic and inelastic contribution $\boldsymbol{F} = \boldsymbol{F}_{e2}\,\boldsymbol{F}_i$ (cf. Fig. 1 b)). The corresponding intermediate configurations ic_1 and ic_2 are introduced according to the aforementioned split of $\boldsymbol{F}$, whereas the elastic right Cauchy-Green tensors and the plastic right Cauchy-Green tensor follow to

$$\boldsymbol{C}_{e1} = \boldsymbol{F}_{e1}^T\,\boldsymbol{F}_{e1} = \boldsymbol{F}_p^{-T}\,\boldsymbol{C}\,\boldsymbol{F}_p^{-1}, \qquad \boldsymbol{C}_{e2} = \boldsymbol{F}_{e2}^T\,\boldsymbol{F}_{e2} = \boldsymbol{F}_i^{-T}\,\boldsymbol{C}\,\boldsymbol{F}_i^{-1}, \qquad \boldsymbol{C}_p = \boldsymbol{F}_p^T\,\boldsymbol{F}_p, \tag{1}$$

respectively.

2.2 Helmholtz free energy

The total Helmholtz free energy is represented by the sum of an elasto-plastic ψ_1, a visco-elastic ψ_2 and a caloric energy contribution ψ_c related to the temperature-dependent specific heat

$$\psi = \psi_1 + \psi_2 + \psi_c. \tag{2}$$

Here, the free energy associated with elastoplasticity

$$\psi_1 = \psi_{e1}(\boldsymbol{C}_{e1}, \chi, \theta) + \psi_p(\boldsymbol{C}_p, \chi, \theta), \tag{3}$$

contains an elastic term

$$\psi_{e1} = \frac{\mu_1}{2}\,(\mathrm{tr}(\boldsymbol{C}_{e1}) - 3) - \mu_1 \ln(J_{e1}) + \frac{\Lambda_1}{4}\,(\det(\boldsymbol{C}_{e1}) - 1 - 2\ln(J_{e1})) - 3\,K_1\alpha_T(\theta - \theta_0)\ln(J_{e1}), \tag{4}$$

based on a Neo-Hookean energy with the two Lamé constants $\mu_1(\theta, \chi)$ and $\Lambda_1(\theta, \chi)$, extended with a term related to the elastic thermal expansion with the coefficient of thermal expansion $\alpha_T(\theta)$ the reference temperature θ_0 and the elasto-plastic bulk modulus K_1. The second term, represents a nonlinear plastic defect energy of Arruda-Boyce type

$$\psi_p = \mu^* \sum_{i=1}^{5} \frac{c_i}{\lambda_m^{2i-1}}(I_{1p}^i - 3^i), \qquad c_i = \left\{\frac{1}{2}, \quad \frac{1}{20}, \quad \frac{11}{1050}, \quad \frac{19}{7000}, \quad \frac{519}{673760}\right\}, \tag{5}$$

depending on the two material parameters $\lambda_m(\theta, \chi)$ and $\mu^*(\theta, \chi)$ (see e.g. [16]), where $I_{1p} = \mathrm{tr}(\boldsymbol{C}_p)$ is the first invariant of the plastic right Cauchy-Green tensor. For the free energy of the visco-elastic part, a Neo-Hookean energy is chosen as well

$$\psi_2 = \frac{\mu_2}{2}\,(\mathrm{tr}(\boldsymbol{C}_{e2}) - 3) - \mu_2 \ln(J_{e2}) + \frac{\Lambda_2}{4}\,(\det(\boldsymbol{C}_{e2}) - 1 - 2\ln(J_{e2})) - 3\,K_2\alpha_T(\theta - \theta_0)\ln(J_{e2}), \tag{6}$$

depending on the viscous Lamé constants $\mu_2(\theta, \chi)$ and $\Lambda_2(\theta, \chi)$ and the determinant of the inelastic deformation gradient $J_{e2} = \det(\boldsymbol{F}_{e2})$. Here, K_2 is the visco-elastic bulk modulus. For a better understanding of the framework and corresponding Helmholtz free energies, a schematic illustration by means of a rheological model is provided in Fig. 1 a).

Function	Parameter at:	23 °C	50 °C	120 °C
$E_1 = \chi E_{1,0}(\theta)$	$E_{1,0}$ [MPa]	7392.6	3016.9	798.26
$E_2 = E_2(\theta)$	E_2 [MPa]	677	639.23	183.6
$\nu_1 = \nu_2$	ν_1 [-]	0.35	0.35	0.35
$\sigma_t = \chi\sigma_{t,0}(\theta)$	$\sigma_{t,0}$ [MPa]	71	49	30
$\sigma_c = \chi\sigma_{c,0}(\theta)$	$\sigma_{c,0}$ [MPa]	284	53.9	30
$\mu^* = \chi\mu_0^*(\theta)$	μ_0^* [MPa]	72	110	114
$\lambda_m = \lambda_m(\theta)$	λ_m [-]	3.6	1.5	2.1
$\tau = \tau(\theta)$	τ [s]	156	71	48

Table 1: Temperature dependent mechanical parameters.

λ_T [W/mK]	c_T [mJ/gK]	ρ_0 [g/mm^3]	α_T [1/K]
0.27	1470000	71	$8.76 \cdot 10^{-5}$

Table 2: Thermal material parameters.

2.3 Derivation based on the Clausius-Duhem inequality

In order to derive thermodynamically consistent constitutive equations and ensure positive dissipation, the Clausius-Duhem inequality

$$\boldsymbol{S} : \frac{1}{2}\dot{\boldsymbol{C}} - \rho_0(\dot{\psi} + \eta\dot{\theta}) - \frac{1}{\theta}\,\boldsymbol{q}_0 \cdot \mathrm{Grad}(\theta) \geq 0, \tag{7}$$

dependent on the density ρ_0, is exploited. Therefore the time derivative of the general Helmholtz free energies (3) and (6) is inserted in (7), yielding

$$\boldsymbol{S} : \frac{1}{2}\dot{\boldsymbol{C}} - \rho_0\left(\frac{\partial\psi}{\partial\boldsymbol{C}_{e1}} : \dot{\boldsymbol{C}}_{e1} + \frac{\partial\psi}{\partial\boldsymbol{C}_p} : \dot{\boldsymbol{C}}_p + \frac{\partial\psi}{\partial\boldsymbol{C}_{e2}} : \dot{\boldsymbol{C}}_{e2}\right) - \rho_0\left(\frac{\partial\psi}{\partial\theta} + \eta\right)\dot{\theta} - \frac{1}{\theta}\boldsymbol{q}_0 \cdot \mathrm{Grad}(\theta) \geq 0. \tag{8}$$

Using the plastic velocity gradient $\boldsymbol{L}_p = \dot{\boldsymbol{F}}_p\boldsymbol{F}_p^{-1}$, the expression can be reformulated, leading to the definition of several stress quantities in line with [3, 17]. The second Piola-Kirchhoff stress tensors $\boldsymbol{S}_1$ and $\boldsymbol{S}_2$, corresponding to the elastoplastic and viscous model contributions, respectively, are introduced as

$$\boldsymbol{S}_1 = 2\rho_0\boldsymbol{F}_p^{-1}\frac{\partial\psi_{e1}}{\partial\boldsymbol{C}_{e1}}\boldsymbol{F}_p^{-T}, \quad \boldsymbol{S}_2 = 2\rho_0\boldsymbol{F}_i^{-1}\frac{\partial\psi_{e2}}{\partial\boldsymbol{C}_{e2}}\boldsymbol{F}_i^{-T}. \tag{9}$$

Whereas the Mandel stress tensors $\boldsymbol{M}_1$ and $\boldsymbol{M}_2$ in the plastic and inelastic intermediate configuration, respectively, follow to

$$\boldsymbol{M}_1 = 2\rho_0\boldsymbol{C}_{e1}\frac{\partial\psi_{e1}}{\partial\boldsymbol{C}_{e1}}, \quad \boldsymbol{M}_2 = 2\rho_0\boldsymbol{C}_{e2}\frac{\partial\psi_{e2}}{\partial\boldsymbol{C}_{e2}}. \tag{10}$$

Finally, the back stress $\boldsymbol{X}$ related to kinematic hardening is given as

$$\boldsymbol{X} = 2\rho_0\boldsymbol{F}_p\frac{\partial\psi_p}{\partial\boldsymbol{C}_p}\boldsymbol{F}_p^T. \tag{11}$$

Inserting the above stated stress measures back into (8) and exploting $\boldsymbol{S} = \boldsymbol{S}_1 + \boldsymbol{S}_2$, yields the reduced form of the Claudius-Duhem inequality

$$(\boldsymbol{M}_1 - \boldsymbol{X}) : \boldsymbol{D}_p + \boldsymbol{M}_2 : \boldsymbol{D}_i \geq 0. \tag{12}$$

Here, the relation $\boldsymbol{D}_{(*)} = \mathrm{sym}\,(\boldsymbol{L}_{(*)})$ for the symmetric part of the corresponding velocity gradient is used. In terms of the thermal contributions, the entropy is defined as $\eta = -\partial\psi/\partial\theta$ and Fouriers's law

$$\boldsymbol{q}_0 = -J\,\lambda_T\,\boldsymbol{C}^{-1}\,\mathrm{Grad}(\theta) \tag{13}$$

is used with $J = \det\boldsymbol{F}$ and $\lambda_T(\theta)$ denoting the temperature dependent heat conductivity.

2.4 Evolution equations

Within the elasto-plastic model contribution a Tschoegl-type yield criterion [18, 19]

$$\Phi_p = 3J_2 + (m-1)\sigma_t I_1 - m\,\sigma_t^2 \leq 0 \tag{14}$$

is used. Including the first $I_1 = \mathrm{tr}(\boldsymbol{M}_1 - \boldsymbol{X})$ and second $J_2 = 1/2\,\mathrm{tr}(\mathrm{dev}(\boldsymbol{M}_1 - \boldsymbol{X}) \cdot \mathrm{dev}(\boldsymbol{M}_1 - \boldsymbol{X}))$ invariant and thus accounting for the effects of hydrostatic pressure on the yielding behavior [20]. A tension-compression flow asymmetry is accounted for via the ratio m

$$m = \frac{\sigma_c(\chi, \theta)}{\sigma_t(\chi, \theta)}, \tag{15}$$

which comprises the yield stresses in tension σ_t and compression σ_c, both dependent on temperature and the degree of crystallinity. With the assumption of associative plasticity, the evolution equation for the plastic part follows to

$$\boldsymbol{D}_p = \dot{\lambda}_p \frac{\partial \Phi_p}{\partial \boldsymbol{M}_1} = \dot{\lambda}_p \Big(3\mathrm{dev}(\boldsymbol{M}_1 - \boldsymbol{X}) + (m-1)\,\sigma_t\,\boldsymbol{I} \Big), \tag{16}$$

where $\dot{\lambda}_p$ denotes the plastic mutiplier. Finally, the Karush-Kuhn-Tucker conditions are stated as

$$\dot{\lambda}_p \geq 0, \quad \Phi_p \leq 0, \quad \dot{\lambda}_p\,\Phi_p = 0. \tag{17}$$

For the viscous model, the evolution equation dependent on the bulk modulus $K_2(\theta)$ as well as the shear modulus $\mu_2(\theta)$, is taken from [17] as

$$\boldsymbol{D}_i = \frac{1}{2\tau\mu_2}\mathrm{dev}(\boldsymbol{M}_2) + \frac{1}{9\tau K_2}\mathrm{tr}(\boldsymbol{M}_2)\boldsymbol{I}. \tag{18}$$

Here, the relaxation time τ is assumed to be constant.

2.5 Thermocoupling

To account for heat generation due to dissipation, the local form of the energy balance is considered to derive the heat generation terms using the definition for the entropy from section 2.3 (see [1]). Here, along the introduction of a caloric energy contribution ψ_c, the specific heat capacity c_T is approximated to be constant, following [21]. Since the parameter identification procedure is done for the isothermal model, the thermocoupling is not explained in more detail, the interested reader is referred to [1].

3 Parameter identification

To identify the model parameters, a staggered identification scheme for the isothermal model based on experiments from [15] is used. Firstly, the elastic properties E_{ges} and ν_{ges} are taken directly from the experimental results for a stretch rate of $\dot{\lambda}_x \approx 0.0005 s^{-1}$. The assumption of a parallel arrangement of elastoplastic and viscous model contributions suggests the use of a constant Poisson's ratio, $\nu_{ges} = \nu_1 = \nu_2$, which is taken from digital image correlation (DIC) data (see [15]). In the same manner , regarding the Young's moduli E_1 and E_2 for the elasto-plastic and visco-elastic part, respectively, are chosen additively as $E_{tot} = \chi E_{1,0} + E_2$. Here, as a simplification in line with [1] the visco-elastic material parameters are chosen indepent of the degree of crystallinity. After the determination of the elastic parameters, the parameters related to plastic effects are determined via a multifitting procedure utilizing the Genetic as well as Downhill-Simplex algorithm in combination with experimental monotonic tension tests. In this way, a parameter set for each temperature is derived, which is simultaneously valid for all degrees of crystallinities. For $23°\mathrm{C}$, $50°\mathrm{C}$ and $120°\mathrm{C}$, the results of the identification procedure and the agreement with the experimental results can be seen in Fig. 2. It can be concluded, that the model works best for temperatures over the glass transition temperature, whereas for example at room temperature the yieling behavior is not captured accurately. Temperatures in between the experimentally tested cases, can be interpolated via cubic spline interpolation [1]. Finally, the parameters for the viscous model part are taken directly from [15] under the assumption of a constant relaxation time τ. The corresponding parameter sets can be found in Tab. 1 and 2. Note here, that the thermal parameters in Tab. 2 are assumed to be independet of temperature and DOC and therefore valid for all simulations.

4 Conclusion and outlook

In this work a constitutive model for polyamide 6 at large strains was derived. After a brief introduction to the modeling of polymers, the corresponding model equations for the elastoplastic as well as viscous model parts were derived in a thermodynamically consistent manner. Here, a fully thermo-coupled set of equations was established, where the degree of crystallinity served as a constant input parameter. In the elastoplastic part, a Tschoegl-type yield criterion was chosen to account for the tension-compression flow asymmetry of the material as well as to allow for the influence of hydrostatic pressure on the yielding behavior. In a final step, after the implementation as a UMAT in the commercial FEM software Abaqus, the model has

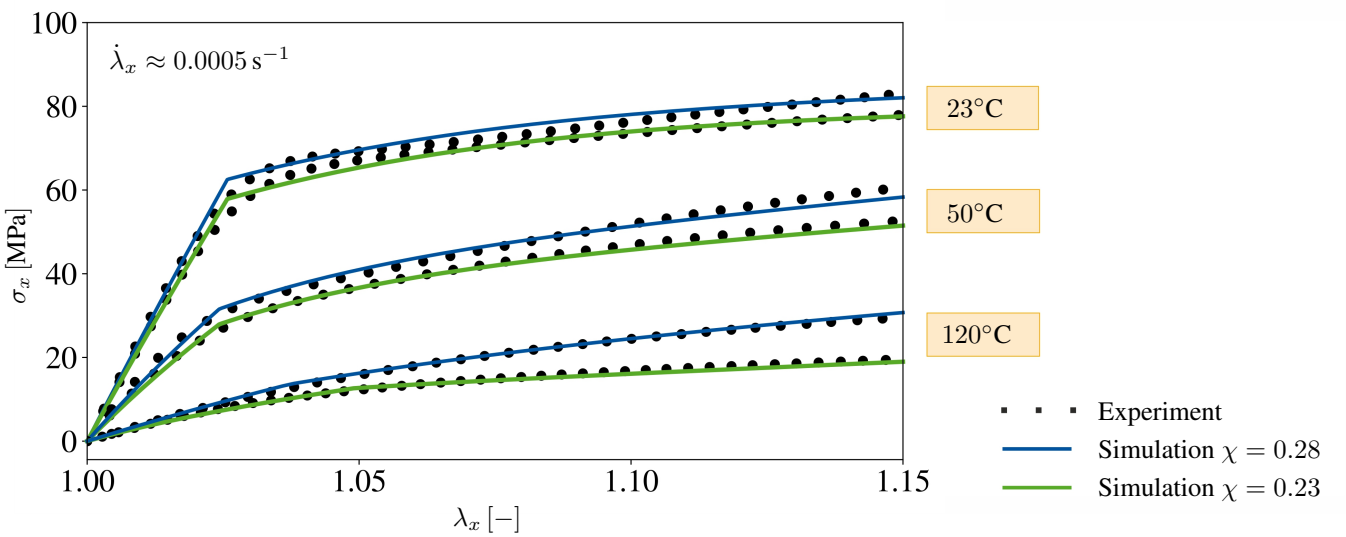

Fig. 2: Monotonic, uniaxial extension: Comparison of experimental data and corresponding model response for 23% and 28% degree of crystallinity at $\dot{\lambda}_x = 0.0005\,s^{-1}$ loading rate.

been characterized using experimental results. Therefore, a staggered parameter identification scheme was exploited to successively identify all needed material parameters. As a result, a parameter set for each individual temperature was found, by taking into account two degrees of crystallinities at the same time. In the future, a model identification with a more extensive experimental study is planned, where a wider range of degrees of crystallinities (approx. $20 - 40\%$) will be accounted for at temperatures between 23 to 150°C. In addition, a function for the relaxation time will be found and compressive tests will be carried out, to identfiy the yield surface fully experimentally. Lastly, the newly characterized material model will be validated with cyclic and structural examples.

Acknowledgements Financial support by the German Research Foundation (DFG) (RE 1057/52-1, project number 454873500) is gratefully acknowledged. In addition, S. Reese acknowledges the funding of the projects RE 1057/46-1 (DFG, project number 404502442) and RE 1057/53-1 (SPP2311) (DFG, project number 465213526) and together with T. Brepols, the financial support for project TRR339 B05 (DFG, project number 453596084). Open access funding enabled and organized by Projekt DEAL.

References

[1] S. Felder, H. Holthusen, S. Hesseler, F. Pohlkemper, T. Gries, J.-W. Simon and S. Reese, Incorporating crystallinity distributions into a thermo-mechanically coupled constitutive model for semi-crystalline polymers, Int. J. Plast., Vol. **135**, pp. 102751 (2020).
[2] L. Anand, N. M. Ames, V. Srivastava and S. A. Chester, A thermo-mechanically coupled theory for large deformations of amorphous polymers. Part I: Formulation., Int. J. Plast., Vol. **25**, pp. 1474–1494 (2009).
[3] I. Vladimirov, M. Pietryga and S. Reese, On the modelling of non-linear kinemtaic hardening at finite strains with application to springback - Comparison of time integration algorithms, Int. J. Numer. Meth. Eng., Vol. **75**, pp. 1–28 (2008).
[4] T. Fornes, D. Paul, Crystallization behavior of nylon 6 nanocomposites, Polym. J., Vol. **44 (14)**, pp. 3945–3961 (2003).
[5] R.N. Haward, G. Thackray, and T.M. Sugden, The use of a mathematical model to describe isothermal stress-strain curves in glassy thermoplastics, Proc. R. Soc. Lond. Ser.A , Vol. **302 (1471)**, pp. 453–472 (1968).
[6] M. Boyce, S. Socrate, and P. Llana, Constitutive model for the finite deformation stress-strain behavior of poly(ethylene terephthalate) above the glass transition, Polym. J. , Vol. **41 (6)**, pp. 2183–2201 (2000).
[7] J.A.W. van Dommelen, D. M. Parks, M. C. Boyce, W.A.M. Brekelmanns and F.P.T. Baaijens, Micromechanical modeling of the elasto-viscoplastic behavior of semi-crystalline polymers, J. Mech. Phys. Solids , Vol. **51 (3)**, pp. 519–541 (2003).
[8] V. Srivastava, S. A. Chester, N. M. Ames and L. Anand, A thermo-mechanically-coupled large-deformation theory for amorphous polymers in a temperature range which spans their glass transition, Int. J. Plast., Vol. **26 (8)**, pp. 1138–1182 (2010).
[9] J. Wang, L.F. Peng, Y.J. Deng, X.M. Lai, M.W. Fu and J. Ni, A finite strain thermodynamically-based constitutive modeling and analysis of viscoelastic-viscoplastic deformation behavior of glassy polymers, Int. J. Plast.,**122**, pp. 135–163 (2019).
[10] G. Ayoub, F. Zaïri, M. Naït-Abdelaziz, J.M. Gloaguen, Modelling large deformation behaviour under loading - unloading of semicrystalline polymers: application to a high density polyethylene. Int. J. Plast., Vol. **26 (3)**, pp. 329–347 (2010).
[11] G. Ayoub, F. Zaïri, C. Fréderix, J. Gloaguen, M. Naït-Abdelaziz, R. Seguela and J. Lefebvre, Effects of crystal content on the mechanical behaviour of polyethylene under finite strains: experiments and constitutive modelling, Int. J. Plast., Vol. **24 (4)**, pp.492–511 (2011).
[12] A. Hassan, N. A. Rahman and R. Yahya, Moisture absorption effect on thermal, dynamic mechanical and mechanical properties of injection-molded short glass-fiber/polyamide 6, 6 composites. Fibers Polym., Vol. **13 (7)**, pp. 899–906 (2012).
[13] D.A. Şerban, G. Weber, L. Marşavina, V.V. Silberschmidt and W. Hufenbach, Tensile properties of semi-crystalline thermoplastic polymers: effects of temperature and strain rates. Polym. Test., Vol. **32 (2)**, pp. 413–425 (2012).

[14] M. Engelhard and A. Lion, Modelling the hydrothermomechanical properties of polymers close to glass transition. Z. Angew. Math. Mech., Vol. **93 (2-3)**, pp. 102–112 (2013).
[15] S. Felder, N. A. Vu, S. Reese and J.-W. Simon, Modeling the effect of temperature and degree of crystallinity on the mechanical response of Polyamide 6, Mech. Mater., Vol. **148**, pp. 103476 (2020).
[16] M. Kaliske and H. Rothert, On the finite element implementation of rubber-like materials at finite strains, Eng. Comput., Vol. **14 (2)**, pp. 216–232 (1997).
[17] S. Reese and S. Govindjee, Theoretical and numerical aspects in the thermo-viscoelastic material behaviour of rubber-like polymers, Mech. Time-Dependent Mater., Vol. **1 (4)**, pp. 357–396 (1998).
[18] N. W. Tschoegl, Failure surfaces in principal stress space, J. Polym. Sci., Vol. **32**, pp. 239–267 (1971).
[19] A. R. Melro, P. P. Camanho, F. A. Pires and S. T. Pinho, Micromechanical analysis of polymer composites reinforced by unidirectional fibres: Part I - Constitutive modelling, Int. J. Solid. Struct., Vol. **50**, pp. 1897–1905 (2013).
[20] E. Ghorbel, A viscoplastic constitutive model for polymeric materials, Int. J. Plast., Vol. **24(11)**, pp. 2032–2058 (2008).
[21] N.M. Ames, V. Srivastava, S.A Chester and L. Anand, A thermo-mechanically coupled theory for large deformations of amorphous polymers. part ii: Applications., Int. J. Plast., Vol. **25(8)**, 1495 –1539 (2009).